# Non-Destructive Detection of Underground Cavities Using Thermal Images

**Nam-jun Cho**

*Professor, Department of Civil and Environmental Engineering, Kookmin University, Seoul, South Korea*

**Wonjun Cha**

*Master student, Department of Civil and Environmental Engineering, Kookmin University, Seoul, South Korea*

**Hyun-Ki Kim**

*Associate Professor(corresponding author), Department of Civil and Environmental Engineering, Kookmin University, Seoul, South Korea*
*geotech@kookmin.ac.kr*

## ABSTRACT

A non-contact and non-destructive geotechnical exploration method is proposed to detect underground cavities in the back of the concrete wall structure by measuring the temporal variations of the wall surface temperature using the infrared camera. The experimental and numerical analyses are conducted to verify the applicability of this method. The results show that the underground cavities covered by the concrete plate which has a thickness thinner than about 10cm can be detected by the temporal variations of the spatial temperature distribution based on the thermal images of the plate surface captured by the infrared camera.

KEYWORDS: Infrared thermograph, infrared camera, retaining wall, surface temperature

## INTRODUCTION

For the safety of retaining structures, the appropriate construction and maintenance of their back fillings and drainage facilities are to be ensured because of the excessive lateral earth pressure by accumulated ground water in the back. Soil erosion caused by damages and deteriorations of the wall drainage systems can develop underground cavity in the back of the wall as illustrated in Fig. 1. Collapse of such a soil cavity can initiate unexpected settlement of the backfill ground and property damages nearby the wall structures. (Lee et al., 2015; Williams-Milano, 2013; SCRD, 2015; Zhiqing et al., 2003; Kim, 2009)

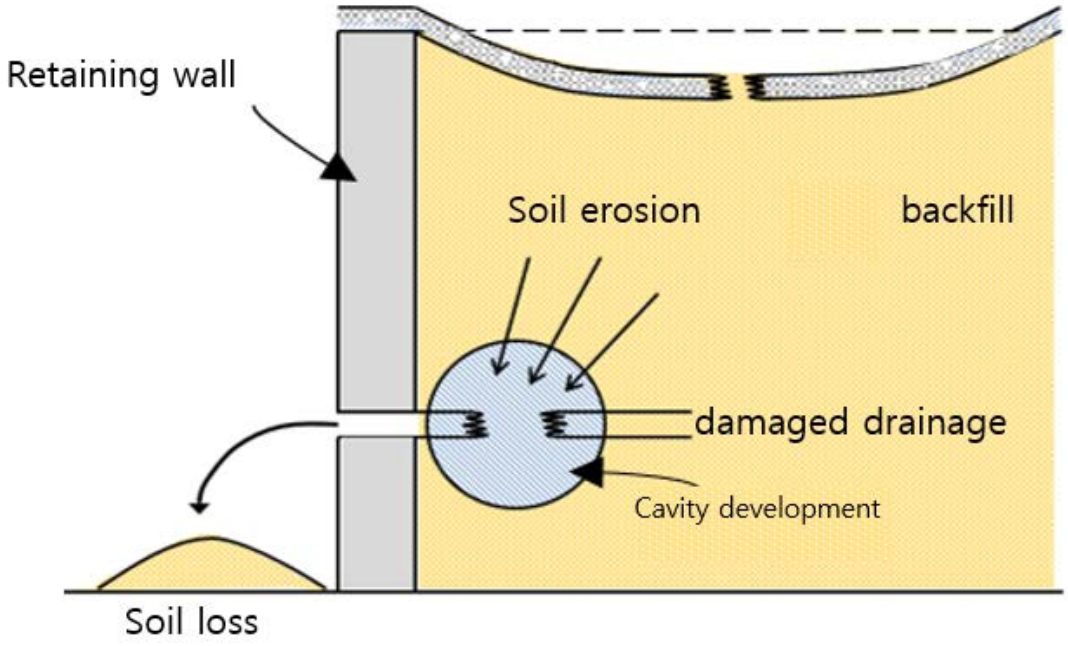


**Figure 1:** Schematic diagram of an underground cavity development at the damaged wall drainage

A number of non-destructive investigation methods, which can be applicable to detect such underground cavities, are already developed (Park et al., 2015; Do et al., 2007): Elastic wave surveys (seismic refraction method, sonar method, surface wave method, ambient vibration measurement, etc. and electromagnetic wave surveys (electric resistivity method, induced polarization method, self-potential method, ground penetration radar, magnetoelectric method, AMT, CSAMT, EM method, etc.). Those techniques are generally based on the elastic or electromagnetic wave propagation through soils. Carefully secured coupling between the transducers and the tested objects should be required to obtain the testing results suitable for the appropriate engineering decision. However, it is not easy to be achieved under usual field measurement conditions and if not, it becomes a main reason for the measurement uncertainty.

In this study, the infrared thermography technique is introduced to identify underground cavities by measuring the temporal variation of the temperature on the concrete wall surface. The infrared thermography technique is a measurement and visualization of the surface temperature of the object for analysis and diagnosis using thermal images captured by infrared cameras. This technique has been used for such various scientific and engineering purposes as weather forecasting, ocean temperature monitoring, safety inspections of building structures and so on (Lee, 2004). Recently, this infrared thermography technique is integrated to geotechnical engineering applications: Detection of the cavity behind the shotcrete wall, structural inspection of concrete retaining walls and shotcrete reinforced slope, monitoring of rock surface weathering, and so on (Guo et al., 2013; Hui, 2012; Choi et al., 2004). The laboratory experiments and numerical simulations are conducted and analyzed as described in the following sections in order to verify this infrared thermography technique.

## EXPERIMENTAL SETUP

A square column shaped polyethylene mold, 50cm wide and 100cm high, is prepared as shown in Figs 2 and 3. The mold is separated into two parts. A set of four pin heaters is instrumented inside the upper part of the mold and each pin heater is located at every corner of the mold and away 10cm from the mold wall. The pin heaters are controlled by the temperature measured at a PT-100 thermometer which is 15cm away from the pin heater to adjust the heating condition. An infrared camera is installed on the top of the upper mold and can capture thermal images of the object through the hole on the top. The features of the camera used in this study are listed in Table 1. The monitored specimen is prepared in the lower part of the mold. In order to simulate a concrete wall structure covering a soil deposit with an underground cavity, the lower space is divided into two with an iron plate. A space is filled with dry standard sand by air pluviation method to have a certain void ratio range between 0.70 and 0.72 and the other space remains empty with air. The top of the specimen is covered with a concrete plate. The covering plates with various thicknesses of 3cm, 5cm, 7cm, 10cm and 20cm are manufactured. The engineering and thermal characteristics of the tested materials are summarized in Tables 3 and 4. T-type thermocouples are attached on the plate surface to measure the surface temperature directly and calibrate the thermal image results. In Figs. 2 and 3, the point A indicates the center of the area, which has an empty space to simulate an underground cavity behind the concrete plate, and the point B indicates the center of the area, which has a sand deposit behind the plate.

The pin heaters are operated to keep the temperature at the PT-100 to be 100 degree in Celsius. It is observed that the surface temperature is not changed much with time after heating about 15 hours and the heating condition is kept three more hours to check the thermal changes, and then the heaters are turned off and the mold and the specimen are cooled down by the room temperature which is about 15 degree in Celsius about 6 hours. The surface temperature of the concrete plate is monitored and recorded during the whole testing process.

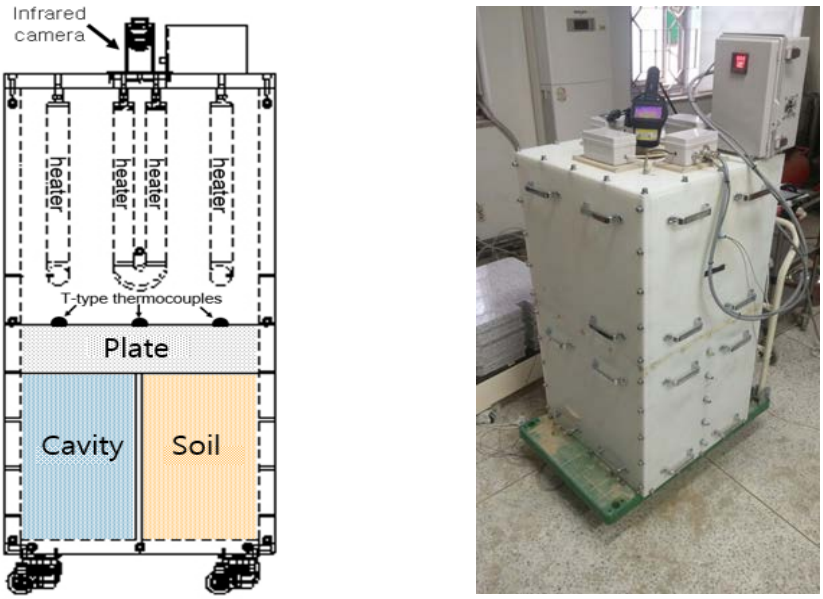


a) Schematic diagram for the testing mold

b) Photograph of the testing mold

**Figure 2:** Schematic diagram and photograph of the testing mold

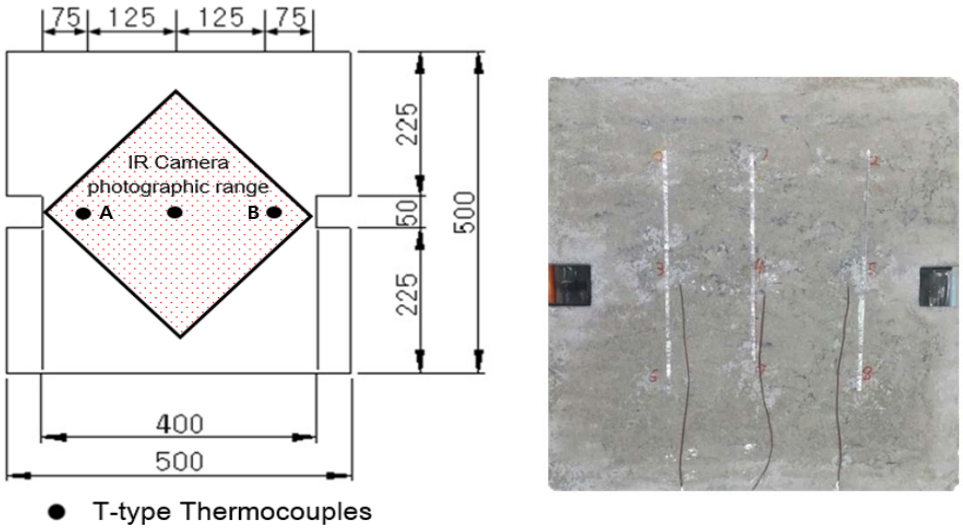


**Figure 3:** Schematic diagram and photograph for the concrete plate

**Table 1:** Characteristics of the infrared camera used in this study (FLIR, 2014)

| | Feature |
|---|---|
| Thermal Image Resolution | 160 X 120 pixels |
| Spatial Sensitivity | 2.72 mrad |
| Temperature Sensitivity | < 0.07℃ |
| Measurable Wavelength | 7.5 ~ 13 ㎛ |
| Measurable Temperature Range | 0℃ ~ 650℃ |

**Table 2:** Engineering Characteristics of the tested sand (Kim, 2014)

| Label | Specific Gravity | Water Content (%) | $D_{50}$ (mm) | $C_u$ | $C_z$ | $e_{max}$ | $e_{min}$ |
|---|---|---|---|---|---|---|---|
| Jumunjin Standard Sand | 2.67 | 0 | 0.56 | 1.53 | 0.94 | 0.92 | 0.60 |

**Table 3:** Thermal properties of the tested materials (after Kim, 2014; Goodfellow, 2015; Johnston, 1981; Peter J. R. and Ann H., 1969)

| | Thermal conductivity (kJ/m·hr·℃) | Volumetric heat capacity (kJ/m$^3$·℃) | Thermal diffusivity (m$^2$s$^{-1}$) |
|---|---|---|---|
| Jumunjin standard Sand | 0.25 ~ 4.00 | 1380 | $0.20 \times 10^{-3}$ ~$2.4 \times 10^{-3}$ |
| Granite (rock) | 6.12 ~ 14.40 | 2128 | $2.87 \times 10^{-3}$ ~$6.77 \times 10^{-3}$ |
| Concrete | 3.60 ~ 6.48 | 2010 | $1.79 \times 10^{-3}$ ~$3.22 \times 10^{-3}$ |
| Polyethylene | 0.33 ~ 0.52 | 1900~2300 | $0.17 \times 10^{-3}$ ~$0.22 \times 10^{-3}$ |
| Air | $0.09 \sim 46.8 \times 10^4$ | 1.26 | $71.43 \times 10^{-3}$ ~$371.43 \times 10^3$ |

## TESTS AND RESULTS

Fig. 4 displays the comparison between experimental and numerical results of temperature changes at the points A and B of the concrete plate during the heating up and the cooling down processes. The temperature distribution during the testing is computed using the computer software TEMP/W (GEO-SLOPE, 2013) and compared with the laboratory testing results as shown in Figs. 4 and 5.

At initial heating, the point A where the cavity is located behind the wall shows a faster build-up of the surface temperature than the point B where soil is filled behind the wall. Then, heat energy loss through the cavity results in a lower temperature at the point A after about 3 hour heating. We confirm no more significant changes in the monitored surface temperature after about 15 hour heating, and then the heaters are turned off and the mold is cooled down with the room temperature which is about 15 degree in Celsius. It is observed that the point A shows much faster temperature drop during this cooling sequence because the more heat energy reserved in the soil deposit rather than the air delays the temperature drop of the area where no cavity is located.

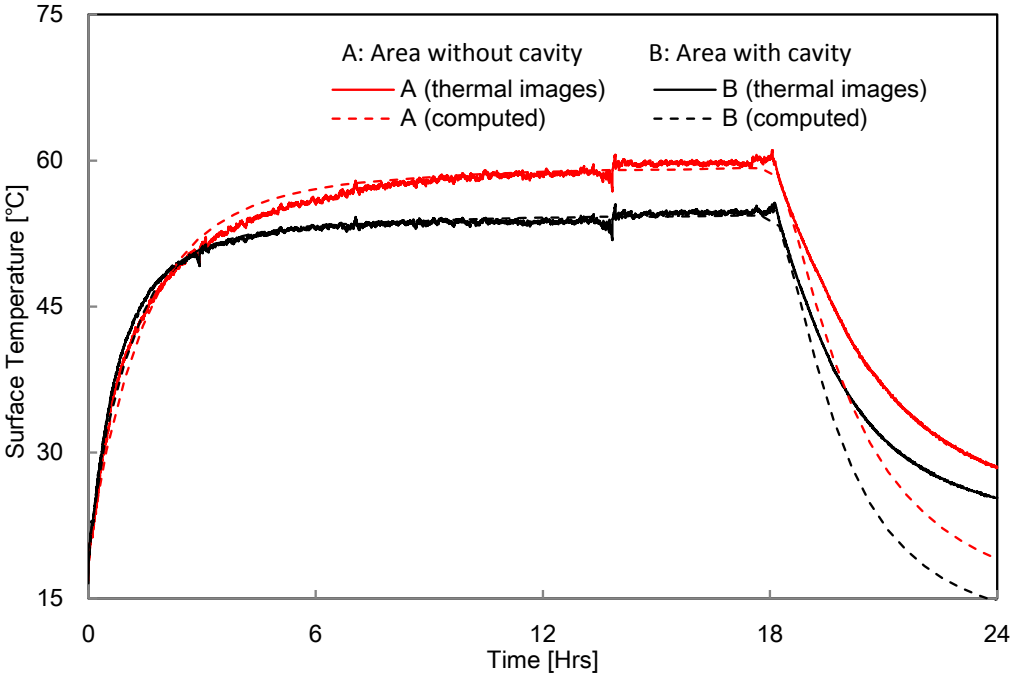


**Figure 4:** Temporal variations of surface temperature at the points A (area without cavity) and B (area with cavity) on the 3cm thick concrete plate

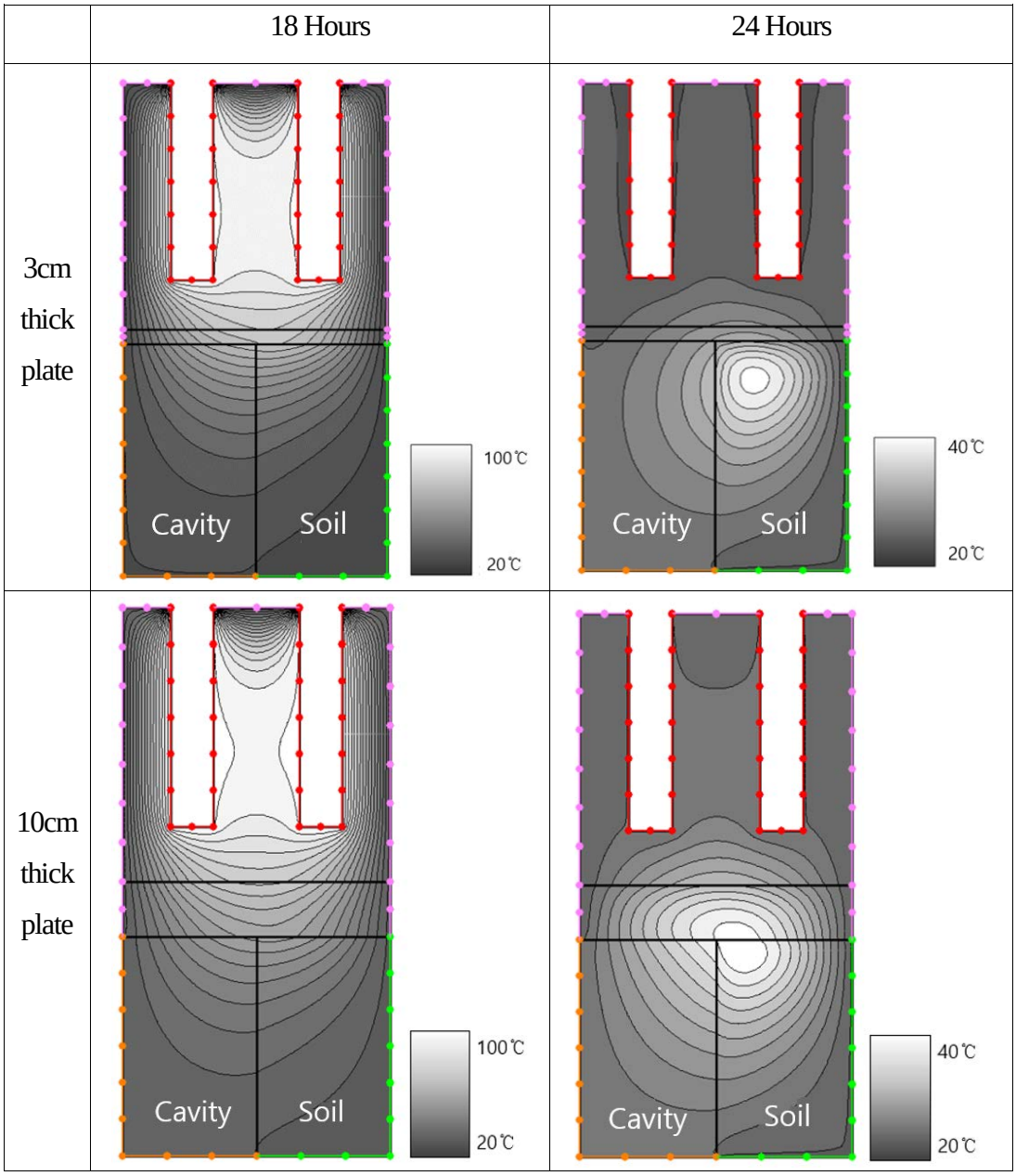


**Figure 5:** Temperature distribution computed using TEMP/W

Fig. 6 shows the temporal variations of the temperature distribution of the concrete plate surface captured by the thermal images. The images show visual discrimination between the areas with the underground cavity and without the cavity: Higher surface temperature on the area without the cavity during both of heating and cooling sequences as discussed previously. Such a visual discrimination of the thermal images can help the engineers to identify underground cavities covered by concrete wall structures.

| | 0 Hours | 2 Hours | 17 Hours | 24 Hours |
|---|---|---|---|---|

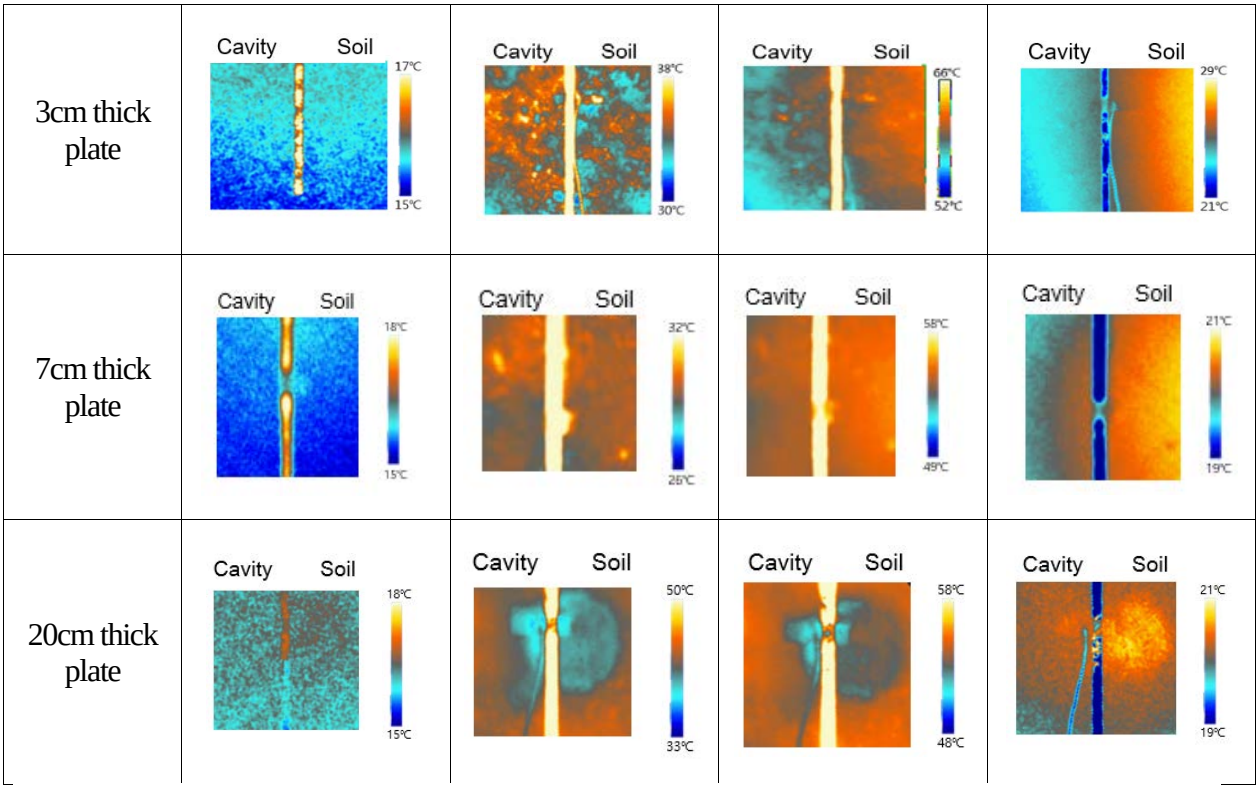


**Figure 6:** Temporal variations of the surface temperature distribution of the concrete plates with different thicknesses captured by the thermal images

Fig. 7 compares the surface temperature measured at the points A and B on the concrete plates with different thickness. Regardless of the concrete plate thickness, the tendency of the surface temperature change with respect to the location of the cavity is the same. However, the thicker plates require more time to be heated to a certain temperature and the surface temperature differences between the points A and B decrease because of overwhelmed thermal diffusion inside the concrete plate.

Fig. 8 displays the surface temperature differences between the points A and B measured at the ends of the heating sequence and the cooling sequence with respect to the concrete plate thickness. During the cooling sequence, the heat energy restored in the soil deposit delays the temperature drop which makes the differences in the surface temperature about 10 to 20% greater than the end of the heating sequence. Simple curves can be drawn to show the effect of the concrete plate thickness on the underground cavity identification as shown together in Fig. 8. This line suggests that such surface temperature measurements can be used as an indicator of an underground cavity covered by the concrete walls thinner than 10cm.

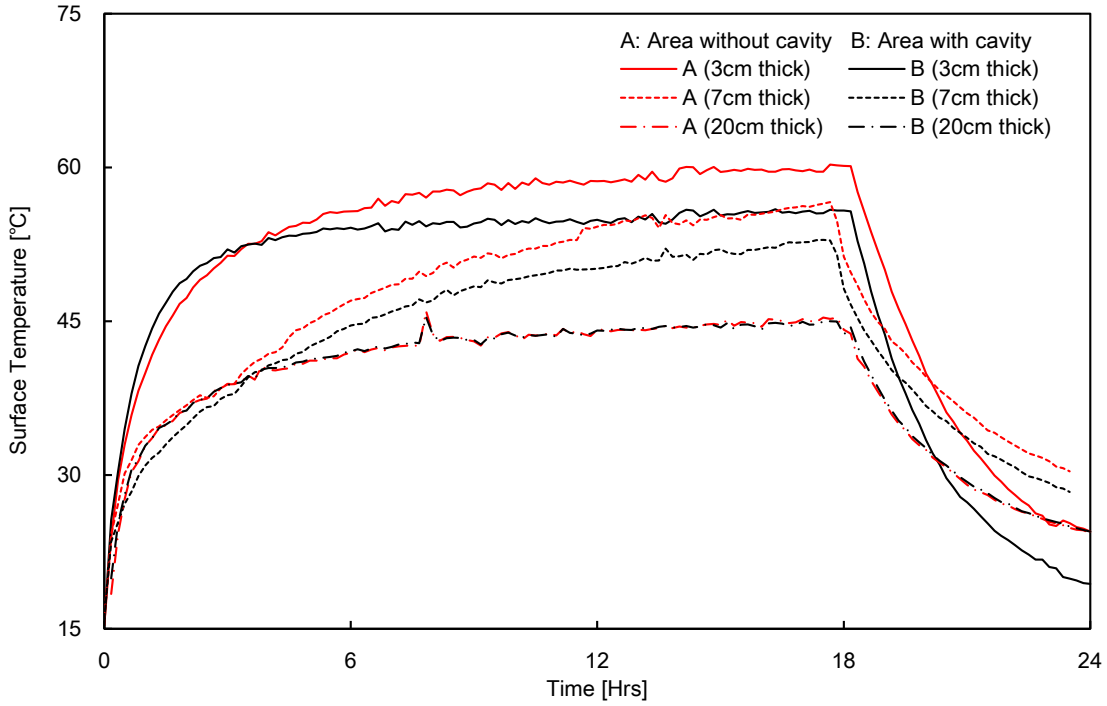


**Figure 7:** Temporal variations of surface temperature for concrete plates with different thicknesses captured by thermal images

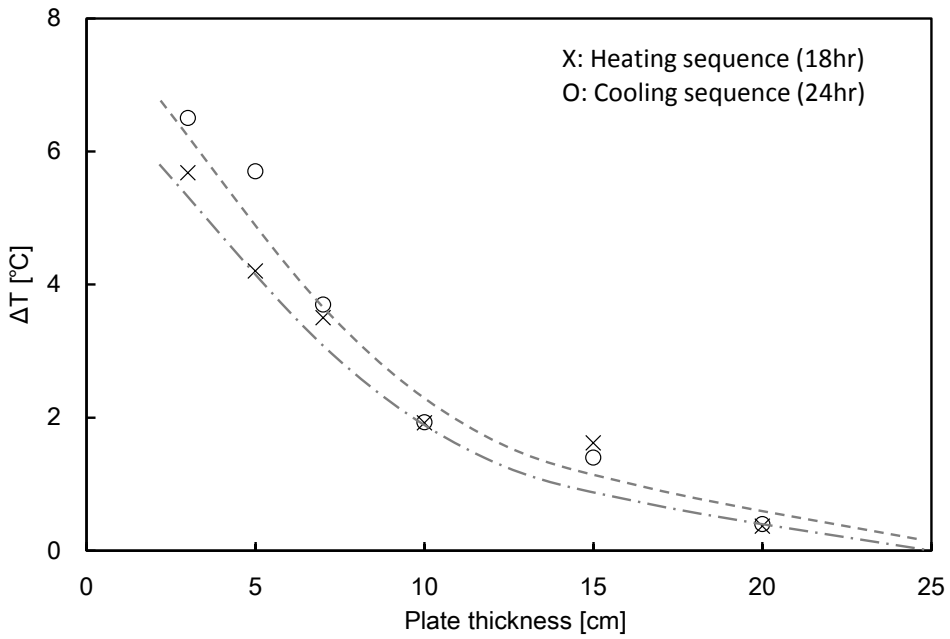


**Figure 8:** Comparison of the maximum surface temperature difference between the points A and B

# CONCLUSIONS

A non-contact and non-destructive geotechnical exploration method is proposed to detect underground cavities in the back of the concrete wall structure by measuring the temporal variations of the wall surface temperature using the infrared camera. For the verification of this method, the experimental and numerical analyses are conducted. The following conclusions can be drawn based on the results.

Differences of thermal characteristics of air and soil deposit bring the spatial differences in surface temperature of the concrete wall covering a soil deposit with an underground cavity. Even exposed to the same heat source, the wall surface covering the underground cavity shows lower temperature than the surface without the cavity behind the wall because of the lower thermal diffusivity of the air in the underground cavity. Such surface temperature differences become greater during the cooling sequence due to the reserved heat energy in the soil deposit.

Such thermal differences with respect to the underground cavity location get reduced with the thicker concrete walls by the overwhelming thermal diffusion inside the wall. Based on the experimental study on the plates with the thickness from 3cm to 20cm, the surface temperature comparison can be an indicator to detect the underground cavities covered by the concrete wall thinner than 10cm in this study.

# ACKNOWLEDGMENTS

This research is supported by a grant (13SCIPS04) from Smart Civil Infrastructure Research Program funded by Ministry of Land, Infrastructure and Transport (MOLIT) of Korea government and Korea Agency for Infrastructure Technology Advancement (KAIA).

# REFERENCES

1. Do, J.N., Lee, C.H., Seo, S.U., and Chun B.S. (2007) A Study on the Effective Cavity Investigation in Limestone area, Korean Society of Civil Engineering, Civil Expo 2007, pp. 731-734
2. FLIR Systems, Inc. (2014) User's manual, FLIR Tools/Tools+, Wilsonville
3. GEO-SLOPE International Ltd. (2013) Thermal Modeling with TEMP/W, Calgary, Alberta, Canada
4. Hui, T. H. H. and Sun H. W. (2005) Trial Application of Thermal Infra-red image and seismic sympathetic vibration techniques for slope investigation, GEO Technical Note No. TN1/200
5. Jang, D.W., Kim, B.S., and Kim J.H. (2012) The Quantification of Disaster Impact of Extreme Rainfall under climate Change in Korea, Journal of Korean Society of Hazard Mitigation, Vol. 12, No.4, pp. 166-178
6. Johnston, G.H. (1981) Permafrost Engineering Design and Construction, Wiley, Toronto, Canada

7. Kim, H.K., Cha, W.J., and Choi, J.W. (2014) A Comparison Study on the Applicability of South Korea Retaining Wall Risk Assessment Method to Urban Area, Journal of Korean Society of Hazard Mitigation, Vol. 14, No.6, pp. 131-139

8. Kim, H.S. (2014) A Study on Subsurface Thermal Diffusion Responses Subject to the Extreme Environmental Conditions, Ph. D Thesis, School of Civil and Environmental Engineering, Kookmin University, Korea

9. Kim, H.S., Cha, W.J., Cho, N.J., and Kim H.K. (2014) Application of Soil Surface Infrared Images for Geotechnical Non-destructive Testing Method, Journal of Korean Society of Hazard Mitigation, Vol. 15, No.3, pp. 249-254

10. Kim, H.W. (2009) A Case Study on the Landslide Resulted from Earth Retaining Wall Failure, International symposium on urban geotchniqe, 2009/9, Incheon, Korea

11. Korean Geotechnical Society. (2009) Foundation Design Criteria , Goomibook, ISBN-978-89-8225-741-4 (93530)

12. Lee, J.Y., Shin, C.G,. Chang, B.S., Son, J.C. (2004) The Non-Destructive and Non-Contact Test Using Infrared Thermal Technique on Reinforced Slopes by Shotcrete, Korean Geotechnical Society, 2004/3, pp.622-628

13. Lee, S.G., Cho, H.K. and Xu, J. (2010) Analysis The Intensity of Weathering of The Rock Surface Using 3D Terrestrial Laser Scanner and Thermal Infrared Instrument, Spring Geoscience 2010/3, Gyunggi, Korea, pp. 1324-1333

14. Lee, S.J., Lee, J.W., Jung, Y.N., Cho, H.J., and Lim, Y.J. (2015) Sensitivity Analysis of the Deformations caused by Cavity Generation in Subway Trackbed Foundation using the FEA, 2015 Fall Conference of the Korean Society for Railway, pp. 1480-1485

15. Park, J.J., Han, J.G., Ryu. S.G., and Hong, G.G. (2015) Current situation of GPR for underground cavity, Korean Geosynthetics Society, Vol. 14, No.3, pp. 12-17

16. Robinson P.J. and Henderson-Sellers A. (1986) Contemporary Climatology, Pearson Education Limited, ISBN 13:978-0-582-27631-4 (pbk)

17. Rees, S.W., Adjali, M.H., Zhou, Z., Davies, M. and Thomas, H.R. (2000) Ground transfer effects on the thermal performance of earth-contact structure, renewable and Sustainable Energy Reviews, Vol. 4, Issue 3, pp.213-265

18. Sunshine Coast Regional District (SCRD), Canada (2015), http://www.scrd.ca/files/File/Community/Building/Retaining-Wall-Stability-and-maintenance%202.pdf

19. Williams-Villano, M. E. (2013), Can your retaining walls withstand the battle of Jericho?, Soil erosion and hydroseeding, Vol. 11, Vo. 1, pp.16-17

20. Zhiqing, W., Siqing, Q., Zhigang, L., & Haitao, Q. (2003) Formation Mechanism and Initial condition of Soil Cavity[J]. Chinese Journal of Rock Mechanics and Engineering, Vol.8

21. Magnetic Method Used In Geothermal Exploration in Ie-Seu ‘Um, Aceh Besar (Indonesia)” *Electronic Journal of Geotechnical Engineering*, 2015 (22.22) pp 12345-12351. Available at ejge.com

22. Muhammad Syukri, Rosli Saad, M.M. Nordiana, and I. N. Azwin: "Preliminary Study of Sumatera Fault Using 2-D Resistivity Imaging Method" *Electronic Journal of Geotechnical Engineering*, 2014: (19/D) pp 971-979. Available at ejge.com.



***Editor's note.***
This paper may be referred to, in other articles, as:

Nam-jun Cho, Wonjun Cha, Hyun-Ki Kim: "Non-Destructive Detection of Underground Cavities Using Thermal Images" *Electronic Journal of Geotechnical Engineering*, 2016 (21.16), pp 5465-5476. Available at **www.**ejge.com**.**